

09 Aug 2017

Defects Classification of Laser Metal Deposition using Acoustic Emission Sensor

Haythem Gaja

Frank W. Liou

Missouri University of Science and Technology, liou@mst.edu

Follow this and additional works at: https://scholarsmine.mst.edu/mec_aereng_facwork



Part of the [Manufacturing Commons](#)

Recommended Citation

H. Gaja and F. W. Liou, "Defects Classification of Laser Metal Deposition using Acoustic Emission Sensor," *Proceedings of the 28th Annual International Solid Freeform Fabrication Symposium (2017, Austin, TX)*, pp. 1952-1964, University of Texas at Austin, Aug 2017.

This Article - Conference proceedings is brought to you for free and open access by Scholars' Mine. It has been accepted for inclusion in Mechanical and Aerospace Engineering Faculty Research & Creative Works by an authorized administrator of Scholars' Mine. This work is protected by U. S. Copyright Law. Unauthorized use including reproduction for redistribution requires the permission of the copyright holder. For more information, please contact scholarsmine@mst.edu.

Defects Classification of Laser Metal Deposition Using Acoustic Emission Sensor

Haythem Gaja*, Frank Liou*⁺

* Mechanical Engineering Missouri University of Science and Technology, Rolla, MO 65409

Abstract

Laser metal deposition (LMD) is an advanced additive manufacturing (AM) process used to build or repair metal parts layer by layer for a range of different applications. Any presence of deposition defects in the part produced causes change in the mechanical properties and might cause failure to the part. In this work, defects monitoring system was proposed to detect and classify defects in real time using an acoustic emission (AE) sensor and an unsupervised pattern recognition analysis. Time domain and frequency domain, and relevant descriptors were used in the classification process to improve the characterization and the discrimination of the defects sources. The methodology was found to be efficient in distinguishing two types of signals that represent two kinds of defects. A cluster analysis of AE data is achieved and the resulting clusters correlated with the defects sources during laser metal deposition.

Keywords: Laser metal deposition, Acoustic emission, Deposition defects, Clustering analysis

INTRODUCTION

In general additive manufacturing is extensively used even though monitoring and detection of defects during AM still require a better understanding. One of the difficulties in using an adaptive control and LMD monitoring system is the accurate detection of defects as being formed during the metal deposition. The objective of monitoring laser metal deposition process is to prevent and detect damage of produced part for any deposition path and part design. In the LMD process, particular changes in the acoustic emission signal indicate the present of defects, these changes must be carefully considered to ensure the effectiveness of the control system. AE has the advantage of real-time, continuous monitoring of LMD. The central goal of such a system is to indicate the occurrence of defects events, but classifying the type of defect is also necessary for the better use of the system and suggestion of corrective remedies.

Bohemen [1] demonstrated that martensite formation during gas tungsten arc (GTA) welding of steel 42CrMo4 can be monitored by means of AE. It was shown that a particular relation exists between the root mean square (RMS) value of the measured AE and the volume rate of the martensite formation during GTA welding. Grad et al. [2] examined the acoustic waves generated during short circuit gas metal arc welding process. It was found that the acoustic method could be used to assess welding process stability and to detect the severe discrepancies in arc behavior.

Yang [3] used an Acoustic emission (AE) sensor to identify damage detection in metallic materials. Results suggested a strong correlation between AE features, i.e., RMS value of the

reconstructed acoustic emission signal, and surface burn, residual stress value, as well as hardness of steels. Diego-Vallejo [4] in his work found that the focus position, as an important parameter in the laser material interactions, changes the dynamics and geometric profile of the machined surface and the statistical properties of measured AE signal.

Recently, Siracusano [5] propose a framework based on the Hilbert–Huang Transform for the evaluation of material damages, this framework facilitates the systematic employment of both established and promising analysis criteria, and provides unsupervised tools to achieve an accurate classification of the fracture type. Bianchi [6] suggested a wavelet packet decomposition within the framework of multiresolution analysis theory is considered to analyze acoustic emission signals to investigate the failure of rail-wheel contact under fatigue and wear study. The application was shown to be an adequate for analyzing such signals and filtering out their noise real time monitoring.

However, more research needs to be done regarding using the acoustic emission sensor in monitoring laser metal deposition. In this paper, the defects type distinguishing of the LMD and its corresponding key features are investigated by clustering the AE signals. The acoustic emission (AE) technique is suitable to examine the defects sources during LMD because of containing rich defect-related information such as crack and pore formation, nucleation and propagation. Information on defects development is difficult to obtain by only using the AE waveform in a time-space, as a non-stationary process, thus other features such as amplitude, energy, rise time, count and frequency are extracted to analyze qualitatively defects mechanisms.

The purpose of the present work is, first to detect laser metal deposition defects as formed layer-by-layer to take the necessary correction action such as machining and remitting, second to develop a reliable method of analysis of AE data during LMD when several AE sources activated to categorize the defects into clusters based on the defect type.

EXPERIMENTAL SETUP

Figure 1 shows a schematic diagram of the experimental set-up. The YAG laser was attached to a 5-Axis vertical computer numerical control machine that is used for post-process machining after LMD. Picoscope 2205A works as a dual-channel oscilloscope to capture the AE signal and stream it to a computer for further analysis, the oscilloscope measures the change in the acoustic emission signal over time, and helps in displaying the signal as a waveform in a graph. An acoustic emission sensor (Kistler 8152B211) captured a high-frequency signal. The bandwidth of the AE sensor was 100 kHz to 1000 kHz. The raw signals were first fed through the data acquisition system and then processed and recorded using Matlab software.

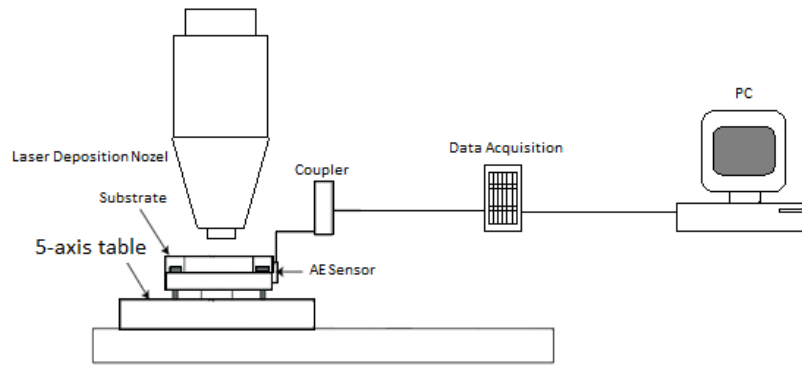
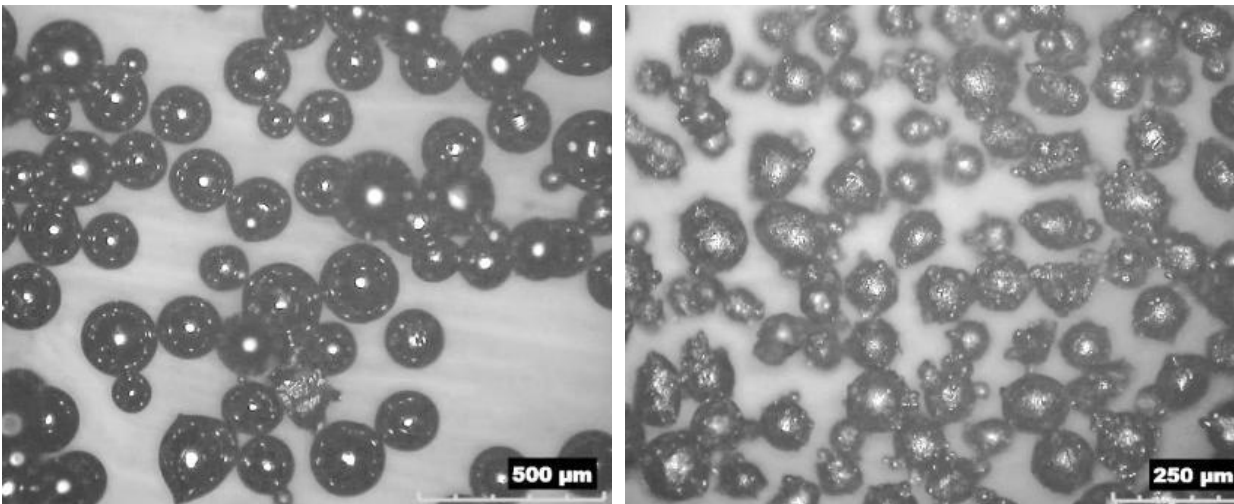


Figure 1. Experimental Setup Shown the LMD System and AE Data Acquisition System

The acoustic emission signal was recorded during a laser deposition process in an oxidized environment and contaminated powder to induce pores and cracks as a result of thermal coefficient difference. The material of the substrate was tool steel. Cracks and porosities were simulated by mixing the mainly Ti-6Al-4V powder with H13 tool steel powder. The two powders particles as illustrated in Figure 2 are non-uniform in shape and size and may contain internal voids which can cause deposition defects when they mixed.



(a) Ti-6Al-4V Metal Powder

(b) H13 Metal Powder

Figure 2 a-b Optical Image of the Metal Powders Used in Deposition Process

Figure 3 illustrate the main steps in the developed procedure which used to analyze the AE data. A layer is created by injecting the metal powder into a laser beam which is used to melt the surface of a substrate and create a small molten pool and generate a deposit. The AE sensor is attached to a substrate to transform the energy released by the laser deposition into acoustic emission signal. The total length of the deposition is 15 mm was performed with standard parameters for depositing titanium powder as shown in Table 1.

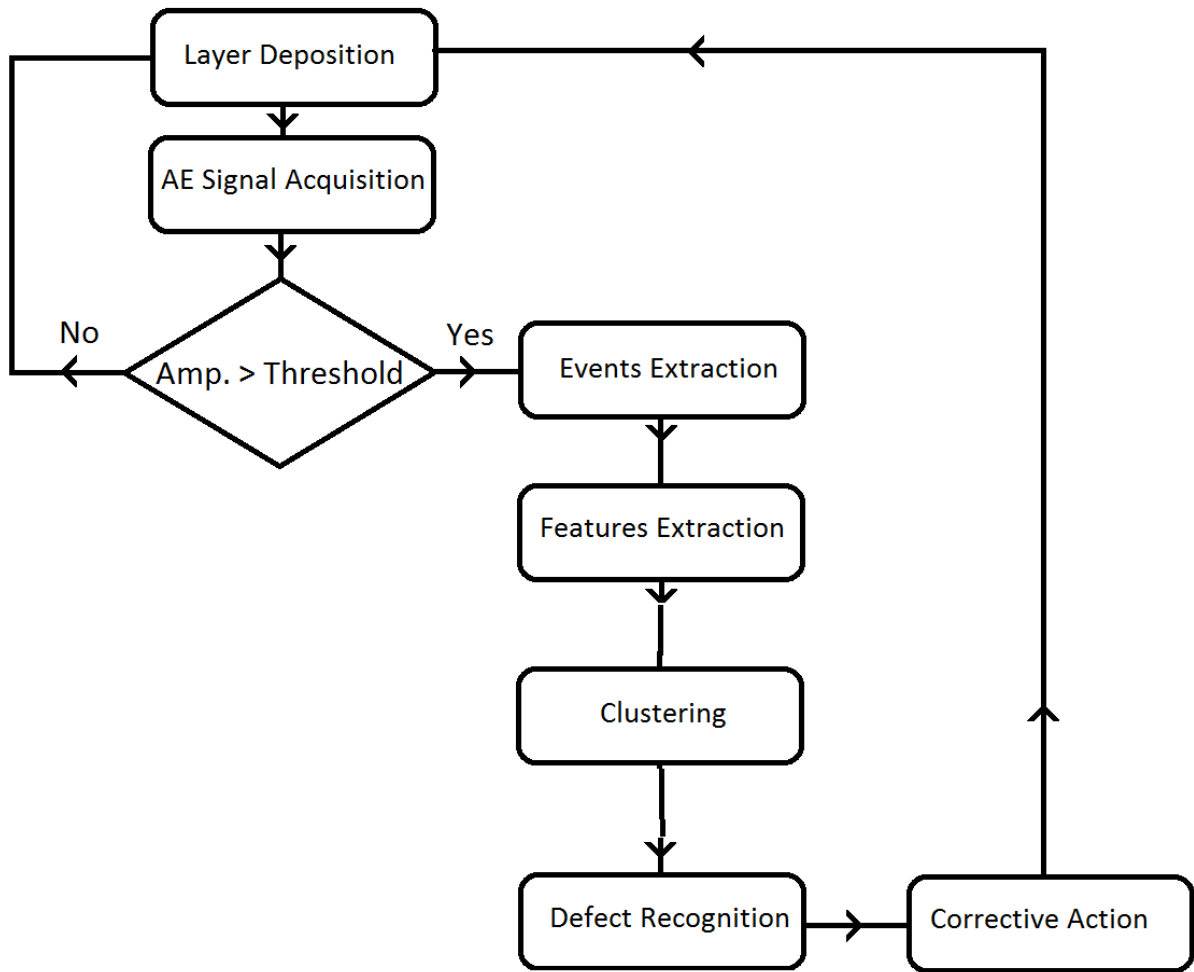


Figure 3. Step-by-step Operations Used to Perform the Acoustic Emission Analyses

Table 1 Laser Metal Deposition process parameters

Parameter	Value
Laser power	1,000 Watt
Powder feed rate	10 g/min
Table velocity	300 mm/min
Length of track	15 mm
Layer thickness	About 0.5 mm
Layer width	About 2.5 mm

The AE events can be represented in the frequency domain using Fast Fourier Transform (FFT) or in the time domain using peak amplitude, kurtosis, energy, the number of counts, duration, and rise time. Among all the features, the signal amplitude alone was measured in real time by the data acquisition system. All the other descriptors were calculated from the waveforms at the end of deposited layer because they are very dependent on the amplitude threshold used to detect the arrival time and the end of an AE signal. Figure 4 shows some of the

time-dependent features. In this work, all these features were used in a multi-parameter statistical analysis and clustering analysis

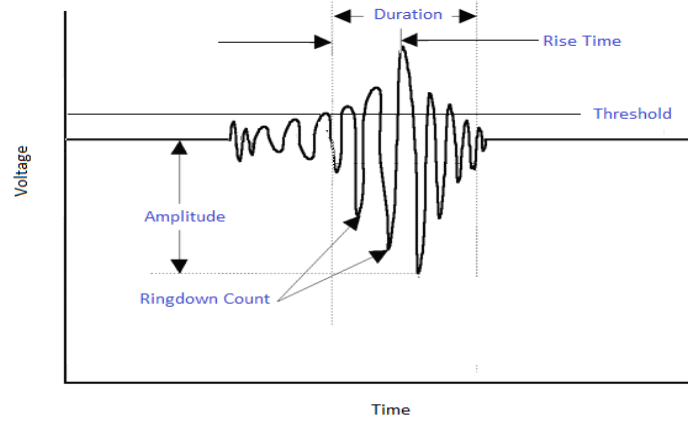


Figure 4 Time dependent AE event features

CLUSTERING ANALYSIS

It is not easy to discriminate precisely the AE signal associated with each defect source from the waveform of the signal; thus, it is useful to use clustering analysis. Clustering analysis is a machine learning technique which group the AE events based on their features to create clusters in such a way that the AE events inside a cluster are similar to each other, and also dissimilar from events in other clusters. In this work, the K-means clustering algorithm was used to group the AE events into homogeneous subgroups (clusters). A silhouette width value was used to find the optimal number of clusters.

The K-means clustering algorithm aims to minimize within-cluster distances between all the vectors of a cluster and its center and maximize the distances between the centers of all clusters. The clustering algorithm requires the number of clusters k to be known and specified in advance; thus, the silhouette width was used for a range of clusters from two clusters to ten clusters. The number of clusters with the maximum average silhouette width was used to group the AE events into sub-groups reflecting the number of defects. The k-means algorithm can then be described as follows:

1. Specify the maximum number of clusters (r).
2. Assume the number of clusters k from 1 to r and randomly initialize each cluster center C_i , where i is from 1 to k
3. Calculate the Euclidean distance between the vector and the centers of the clusters and then assign each input vector (or pattern) to the nearest cluster.
3. Recalculate the location of the cluster center according to the nearest mean.
4. Repeat steps 2 and 3 until there are no changes in these center locations.

5. calculate the maximum average silhouette width.
6. Repeat steps from 2 to 5 for all possible number of clusters.

The greater the silhouette value, the better the clustering results [7, 8]. The optimal value of k is determined according to the maximum of the silhouette width defined as

$$s(k) = \frac{1}{n} \sum_{l=1}^n \frac{\min(b(l,k) - a(l))}{\max(a(l), \min(b(l,k)))} \quad (7)$$

Where $a(l)$ is the average distance between l -th event and all other events in the same cluster, and $b(l, k)$ is the minimum of the average distances between the l -th event and all the event in each other cluster. The silhouette width values range from -1 to 1. If the silhouette width value for an event is about zero, it means that that the event could be assigned to another cluster. If the silhouette width value is close to -1, it means that the event is need to be assigned to other cluster. If the silhouette width values are close to 1, it means that the event is well clustered. A clustering can be evaluated by the average silhouette width $s(k)$ of individual events.

The largest average silhouette width, over different K , indicates the best number of clusters. As can be seen, in Table 2 the greatest average silhouette width is 0.8108. The number of clusters was confirmed using Bayesian Information Criterion (BIC) [9], since it is recommended to validate number of clusters through use of several methods. The number of clusters with the lowest BIC is preferred which means $k=2$ is the optimum number of clusters.

Table 2. Average Silhouette Width for Different Number of Clusters

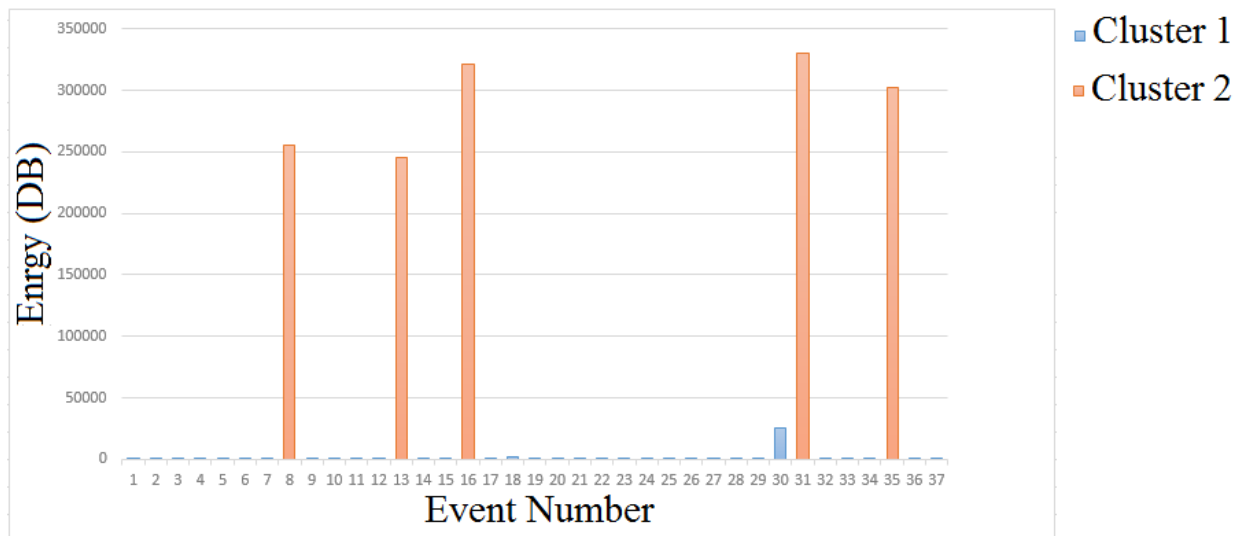
Number of clusters	Average Silhouette Width	BIC
2	0.8108	4409.199532
3	0.4730	5307.464994
4	0.4963	6268.570481
5	0.4770	7268.886407
6	0.5405	8331.531180
7	0.5004	9397.995038
8	0.4387	10464.458896
9	0.5210	11532.648846
10	0.4254	12645.626117
11	0.5346	13763.722664

The defects in cluster two tend to have more energy, longer duration, slower rise time, large number of counts, higher amplitude, close to the normal distribution with flatter and light tail distribution, and less frequency compared to the defects in cluster one.

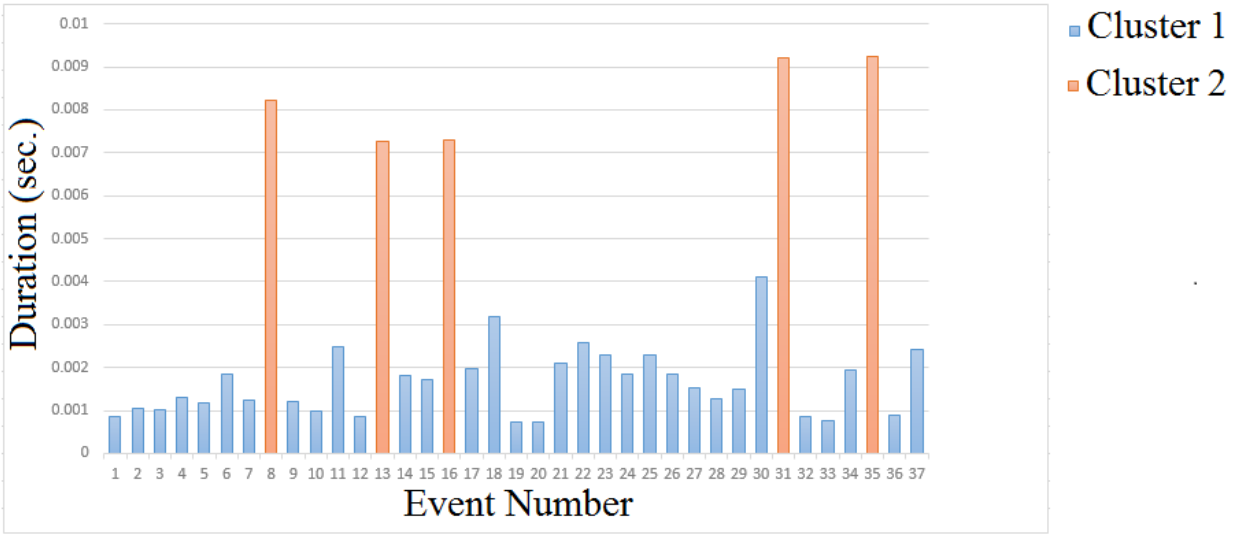
Analysis of variance (ANOVA) of the cluster centers (Table 3). As can be seen, most of the means of clustering features differ significantly across the two clusters, because the null hypothesis (means are equal) is rejected in a case at significant level ≤ 0.05 . The frequency is not significant which means it has a little contribution to the cluster solution. The features with large F value provide the greatest separation between clusters. As the F value increases as the importance of feature increases, this was also illustrated in Figure 5.

Table 3. Analysis of variance (ANOVA) of the cluster centers and features importance

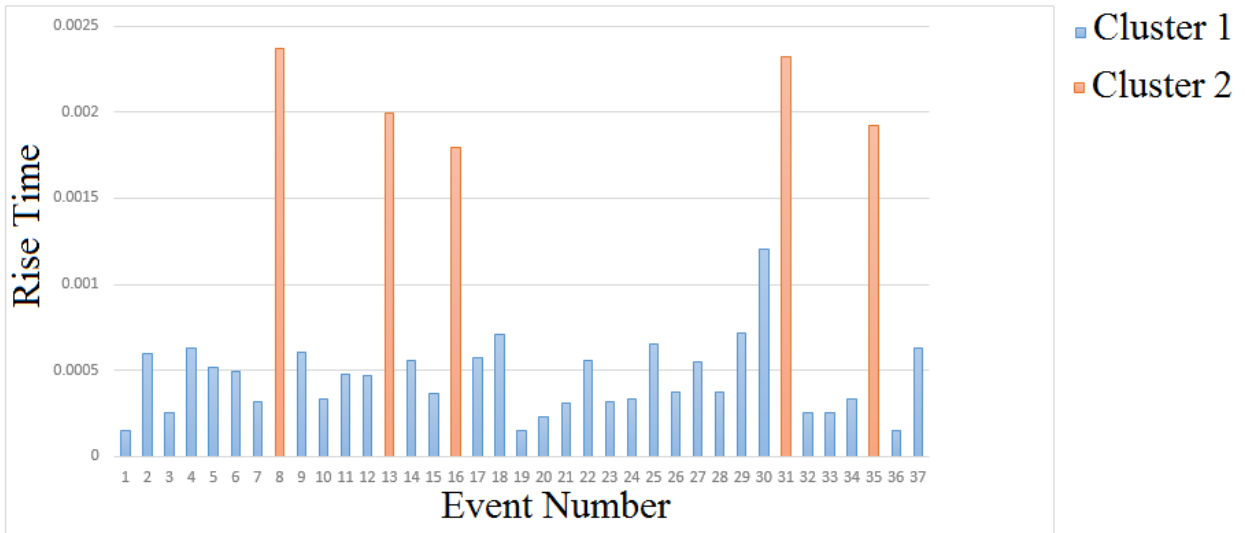
	Cluster		Error		F	Sig.	importance
	Mean Square	df	Mean Square	df			
Rise Time	30.629	1	.153	35	199.608	.000	3
Peak amplitude	29.703	1	.180	35	165.109	.000	5
Duration	30.801	1	.149	35	207.352	.000	2
Kurtosis	3.449	1	.930	35	3.709	.062	9
Number of counts	30.043	1	.170	35	176.523	.000	4
Counts to peak	28.444	1	.216	35	131.750	.000	6
Energy	31.137	1	.139	35	224.074	.000	1
Average frequency	1.184	1	.995	35	1.190	.283	10
Maximum frequency	10.870	1	.718	35	15.140	.000	8
Standard deviation of frequencies	12.417	1	.674	35	18.429	.000	7



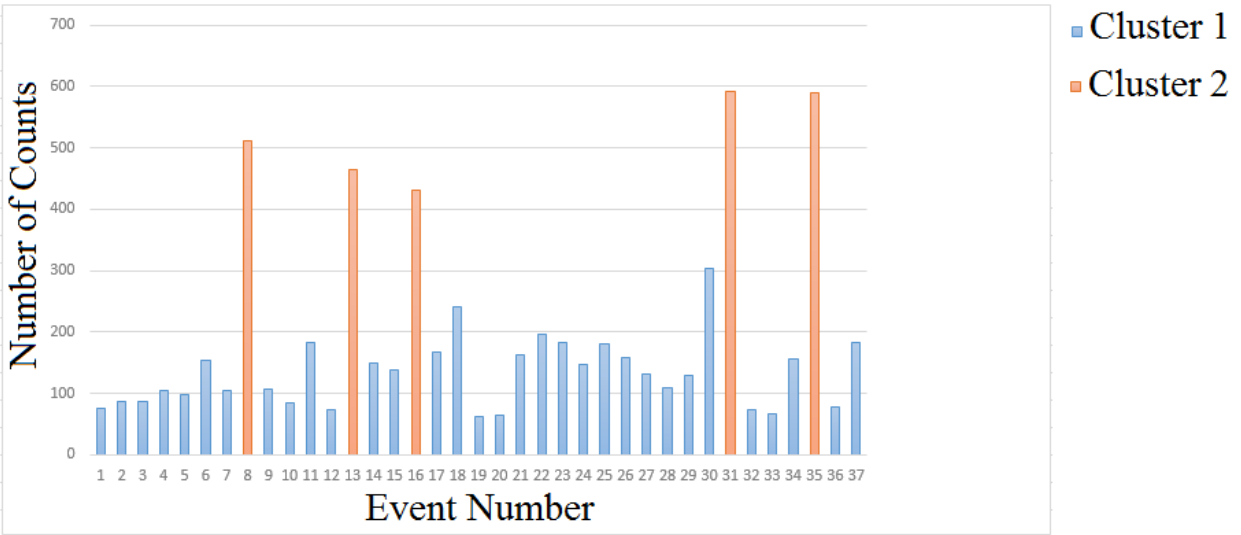
(a) Events in cluster one have less energy



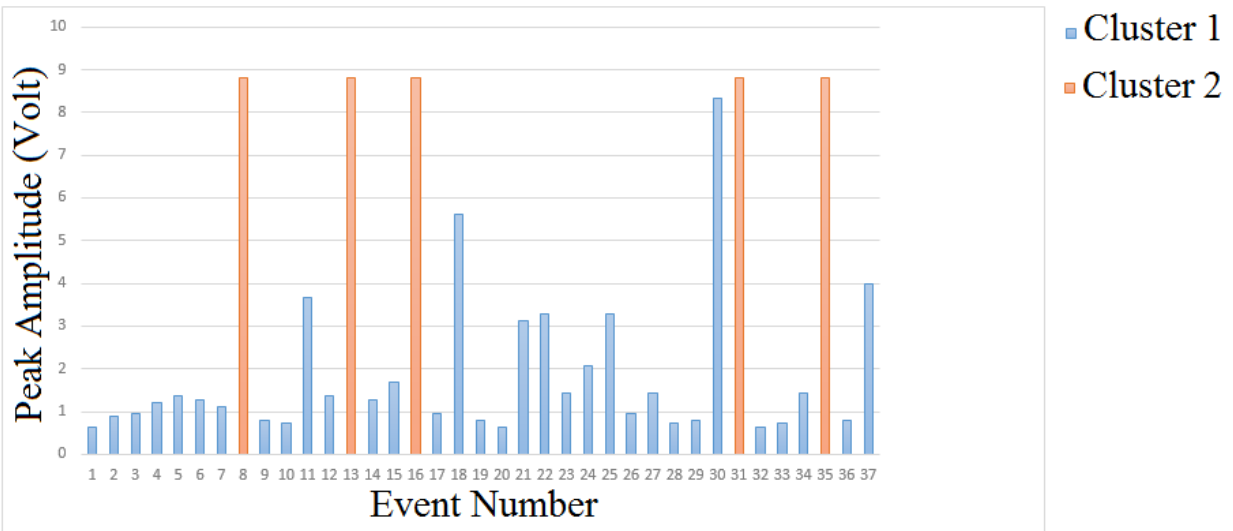
(b) Events in cluster one have shorter duration



(c) Events in cluster one have slower rise time



(d) Events in cluster one have less number of counts

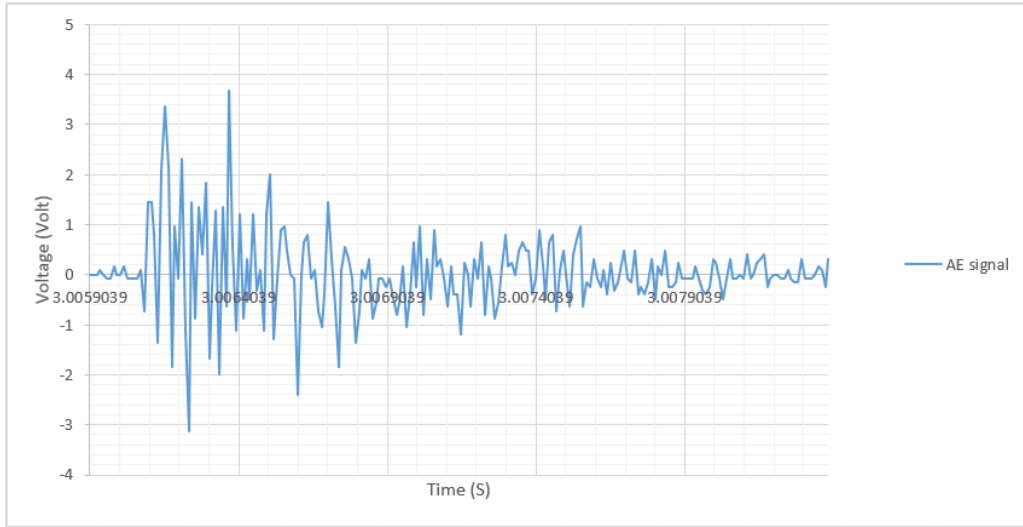


(e) Events in cluster one have lower amplitude

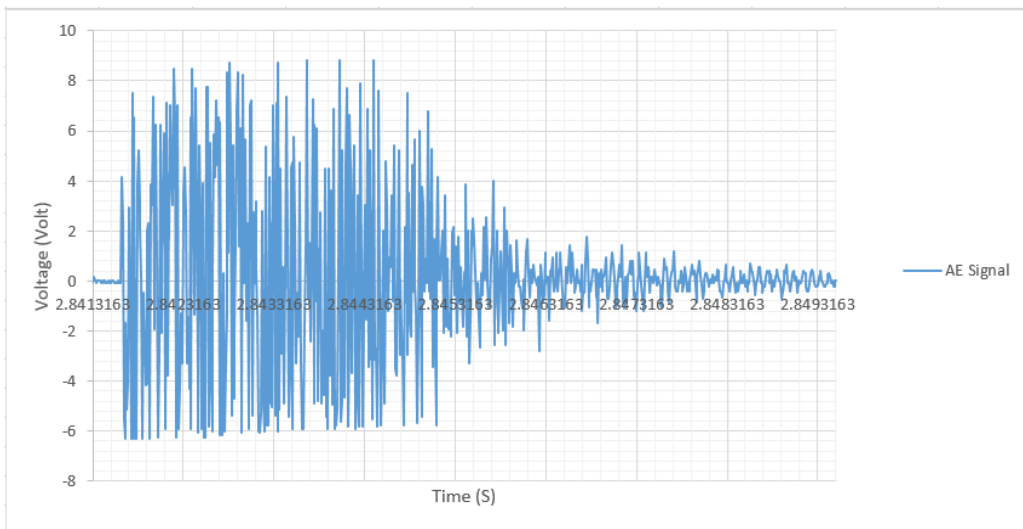
Figure 5 a-e comparing the features in clusters one and two the AE Events

DEFECTS TYPES AND OPTICAL MICROSCOPY STUDY

Figure 6 shows waveform samples from cluster one and cluster two. The waveform from cluster one is quite different from the waveform from cluster two. The dissimilarities in the events features and waveforms found between the two types of signals lead to the conclusion that the source mechanisms are not the same in both cases.



(a) Waveform Signal Sample from Cluster One



(b) Waveform Signal Sample from Cluster Two

Figure 6 a-b Comparison between the Waveforms from both Clusters

After preparing the surface of deposited metal, the cracks and pores were observed using an optical microscope, the number of cracks to the number of pores strongly correlated with the number of events in cluster two to the number of events in cluster one. Also from the literature [10], [11] the waveform and the features of the acoustic emission signal created by cracks is similar to the events in cluster two.

Figure 7 displays cracks caused by thermal stress. The temperature gradient of the deposited layer is large in the direction of thickness during laser deposition process, and the thermal expansion coefficients of the two deposition materials are different, which results in that

the thermal stress at the combining surface of deposition, thus the cracks are formed. It also occurs with powder contamination in the powder feeder [12].

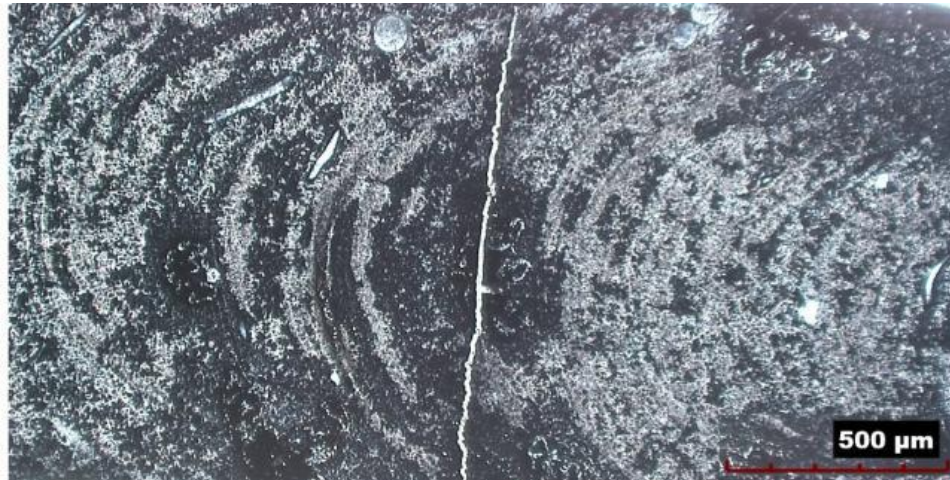


Figure 7 Optical image of a transverse cross-sectioned laser deposit showing a crack and gas porosity

The second type of observed defects is pores which have a spherical form and appear in random locations not associated with the microstructure as shown in Figure 8. The possible sources of these porosities are surface powder contamination [11], gasses trapped within the powder particles due to the difference in the powder sizes, and an oxidation effect since the oxygen level was high due not using the chamber to stimulate defect formation in this research. In fact, surface oxides may most likely remain in the solid state in the melting pool and, as such, upset the wetting mechanisms melted the powder and induces voids.

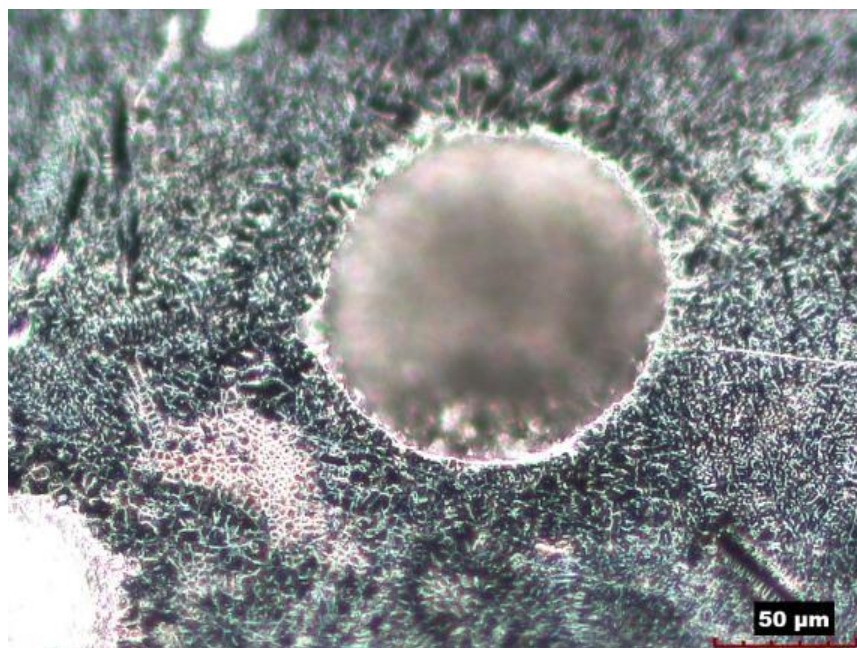


Figure 8 Optical image of a transverse cross-sectioned laser deposit showing a gas porosity

Conclusions

The AE signal was collected during the LMD in an oxidized environment with mixed metal powders to stimulate all possible types of defects. Several defects mechanism were activated and detected by AE sensor. K-Means clustering method was implemented to analyze the AE signals and identify defects source mechanisms.

The clustering results successfully distinguish two main defects types and their signal characteristics. The number of clusters to be created does not have to be specified in advance, they only depend on the number of defects being created. Porosities produce the AE signals with shorter decay time and less amplitude. The cracks trigger the AE signals with short durations and high amplitudes. The signal energy is a crucial feature in identifying the AE defect source mechanisms.

The validation of the proposed methodology has been carried out using an optical microscope; it showed the correlation between the number of acoustic events and the number of defects determined by post-test optical microscopy. The numbers of signal events in each cluster are in agreement with the rough estimations of the associated numbers of defects.

REFERENCES

- [1] Van Bohemen, S M C; Hermans, M J M; Den Ouden, G.,” Monitoring of martensite formation during welding by means of acoustic emission “, Journal of Physics D, Applied Physics (UK) 34.22 (21 Nov. 2001): 3312-3317.
- [2] L.Grad, J.Grum, I. Polajnar and J.M.Slabe, “Feasibility study of acoustic signals for on-line monitoring in short circuit gas metal arc welding”, International Journal of Machine Tools and Manufacture, Volume 44, Issue 5, April 2004
- [3] Yang, Z., Yu, Z., Wu, H., & Chang, D. (2014). “Laser-induced thermal damage detection in metallic materials via acoustic emission and ensemble empirical mode decomposition”, Journal of Materials Processing Technology, 214(8), 1617-1626.
- [4] D. Diego-Vallejo, D. Ashkenasi, H.J. Eichler, “Monitoring of Focus Position During Laser Processing based on Plasma Emission, Physics Procedia”, Volume 41, 2013
- [5] Giulio Siracusano, Giovanni Finocchio, “A framework for the damage evaluation of acoustic emission signals through Hilbert–Huang transform”, Mechanical Systems and Signal Processing, Volume 75, 15 June 2016
- [6] Davide Bianchi, András Vernes, ‘Wavelet packet transform for detection of single events in acoustic emission signals’, Mechanical Systems and Signal Processing, Volumes 64–65, December 2015, Pages 441-451
- [7] R. Gutkin, C.J. Green, S. Vangrattanachai, S.T. Pinho, P. Robinson, P.T. Curtis, On acoustic emission for failure investigation in CFRP: Pattern recognition and peak frequency analyses, Mechanical Systems and Signal Processing, Volume 25, Issue 4, May 2011, Pages 1393-1407
- [8] Peter J. Rousseeuw, Silhouettes: A graphical aid to the interpretation and validation of cluster analysis, Journal of Computational and Applied Mathematics, Volume 20, 1987, Pages 53-65
- [9] Dan Pelleg, Andrew W. Moore. 2000. “X-means: Extending K-means with Efficient Estimation of the Number of Clusters.” Proceedings of the Seventeenth International Conference on Machine Learning. 2000, 727-734.
- [10] F. Arcella, F. Froes, Producing titanium aerospace components from powder using laser forming, JOM 52 (2000) 28–30.
- [11] Lu, S. P., et al. "Acoustic emission monitoring and microscopic investigation of cracks in ERCuNi cladding." J. Mater. Sci. Technol. 19.3 (2003): 201-205.
- [12] Barua, S., et al., 2014, "Vision-Based Defect Detection in Laser Metal Deposition Process," Rapid Prototyping Journal, 20(1): p. 77-85.